ILC2s regulate adaptive Th2 cell functions via PD-L1 checkpoint control

Christian Schwartz,[1,2] Adnan R. Khan,[1,2] Achilleas Floudas,[1,2] Sean P. Saunders,[1,2] Emily Hams,[1,2] Hans-Reimer Rodewald,[3] Andrew N.J. McKenzie,[4] and Padraic G. Fallon[1,2,5]

[1]Trinity Biomedical Sciences Institute, School of Medicine and [2]Trinity Translational Medicine Institute, Trinity College Dublin, Dublin, Ireland
[3]Division of Cellular Immunology, German Cancer Research Center, Heidelberg, Germany
[4]Medical Research Council Laboratory of Molecular Biology, Cambridge, UK
[5]National Children's Research Centre, Our Lady's Children's Hospital, Crumlin, Dublin, Ireland

Group 2 innate lymphoid cells (ILC2s) are important effector cells driving the initiation of type 2 immune responses leading to adaptive T helper 2 (Th2) immunity. Here we show that ILC2s dynamically express the checkpoint inhibitor molecule PD-L1 during type 2 pulmonary responses. Surprisingly, PD-L1:PD-1 interaction between ILC2s and CD4$^+$ T cells did not inhibit the T cell response, but PD-L1–expressing ILC2s stimulated increased expression of GATA3 and production of IL-13 by Th2 cells both in vitro and in vivo. Conditional deletion of PD-L1 on ILC2s impaired early Th2 polarization and cytokine production, leading to delayed worm expulsion during infection with the gastrointestinal helminth *Nippostrongylus brasiliensis*. Our results identify a novel PD-L1–controlled mechanism for type 2 polarization, with ILC2s mediating an innate checkpoint to control adaptive T helper responses, which has important implications for the treatment of type 2 inflammation.

The Journal of Experimental Medicine

INTRODUCTION

Innate lymphoid cells (ILCs) are now recognized as important regulators of multiple facets of immunity, spanning host defense, inflammation, metabolic homeostasis, and tissue repair (Flach and Diefenbach, 2015; ; Sonnenberg and Artis, 2015; Klose and Artis, 2016; Monticelli et al., 2016). ILCs provide the initial innate cellular responses, normally within mucosal barriers, that initiate and orchestrate systemic adaptive immunity (Klose and Artis, 2016). Group 2 ILCs (ILC2s) were first discovered as the cell sentinels responding to helminth worm infection that evoked the generation of adaptive type 2 immunity, which functioned in mediating worm rejection, allergic immunity, and repair and resolution of tissue damage (Fort et al., 2001; Fallon et al., 2006; Moro et al., 2010; Neill et al., 2010; Price et al., 2010; Saenz et al., 2010). They are predominantly found at mucosal barriers, such as human and mouse lungs, where they play roles in the initiation of protective immunity, and as effector cells during allergen-induced type 2 airway inflammation, virus infection, and antiparasite responses (Monticelli et al., 2011; Halim et al., 2012; Gorski et al., 2013). ILC2s are activated by the alarmins IL-33, IL-25, and thymic stromal lymphopoietin, which are released during tissue injury (Kim et al., 2013; Salimi et al., 2013). Upon activation, ILC2s release large amounts of type 2 cytokines IL-5 and IL-13, and also IL-4, as well as IL-9 and amphiregulin, which contribute to tissue repair (Turner et al., 2013; Monticelli et al., 2015).

There is emerging evidence that ILC2s or ILC3s can directly influence Th cell polarization and functions (Hepworth et al., 2013, 2015; Mirchandani et al., 2014; von Burg et al., 2015). It has been recently described that ILC2s express MHC class II molecules and can augment Th2 polarization (Oliphant et al., 2014; Halim et al., 2016). Furthermore, ICOS and ICOS-L are activating coreceptors shown to be present on ILC2s (Maazi et al., 2015). The engagement of PD-1, primarily expressed on T cells, via its ligands PD-L1 and PD-L2 delivers an inhibitory signal to the PD-1–bearing cell (Agata et al., 1996; Freeman et al., 2000; Latchman et al., 2001; Barber et al., 2006). Inhibition via PD-1 engagement enables tumor cells to keep the adaptive immune response in check, and we have shown that parasites such as *Schistosoma mansoni* also use PD-L1–mediated immunosuppression to evade the adaptive immune system (Smith et al., 2004; Keir et al., 2008; Khan et al., 2015). Although described as an inhibitory interaction partner of PD-1, evidence also supports an activating function for PD-L1 (Liechtenstein et al., 2012). During *Listeria monocytogenes* infection, PD-L1 delivers positive costimulatory signals to innate and adaptive immune cells to protect from intracellular infection (Seo et al., 2008). PD-1 engagement can generate induced regulatory T cells, and PD-L1 costimulates T cell responses against polyclonal stimuli (Dong et al., 1999; del Rio et al., 2005; McAlees et al., 2015). So far, little is known of the involvement of PD-L1 in the control of strong type 2 immune responses.

Correspondence to Padraic G. Fallon: pfallon@tcd.ie

Abbreviation used: ILC, innate lymphoid cell.

The Rockefeller University Press
J. Exp. Med. 2017 Vol. 214 No. 9 2507–2521
https://doi.org/10.1084/jem.20170051

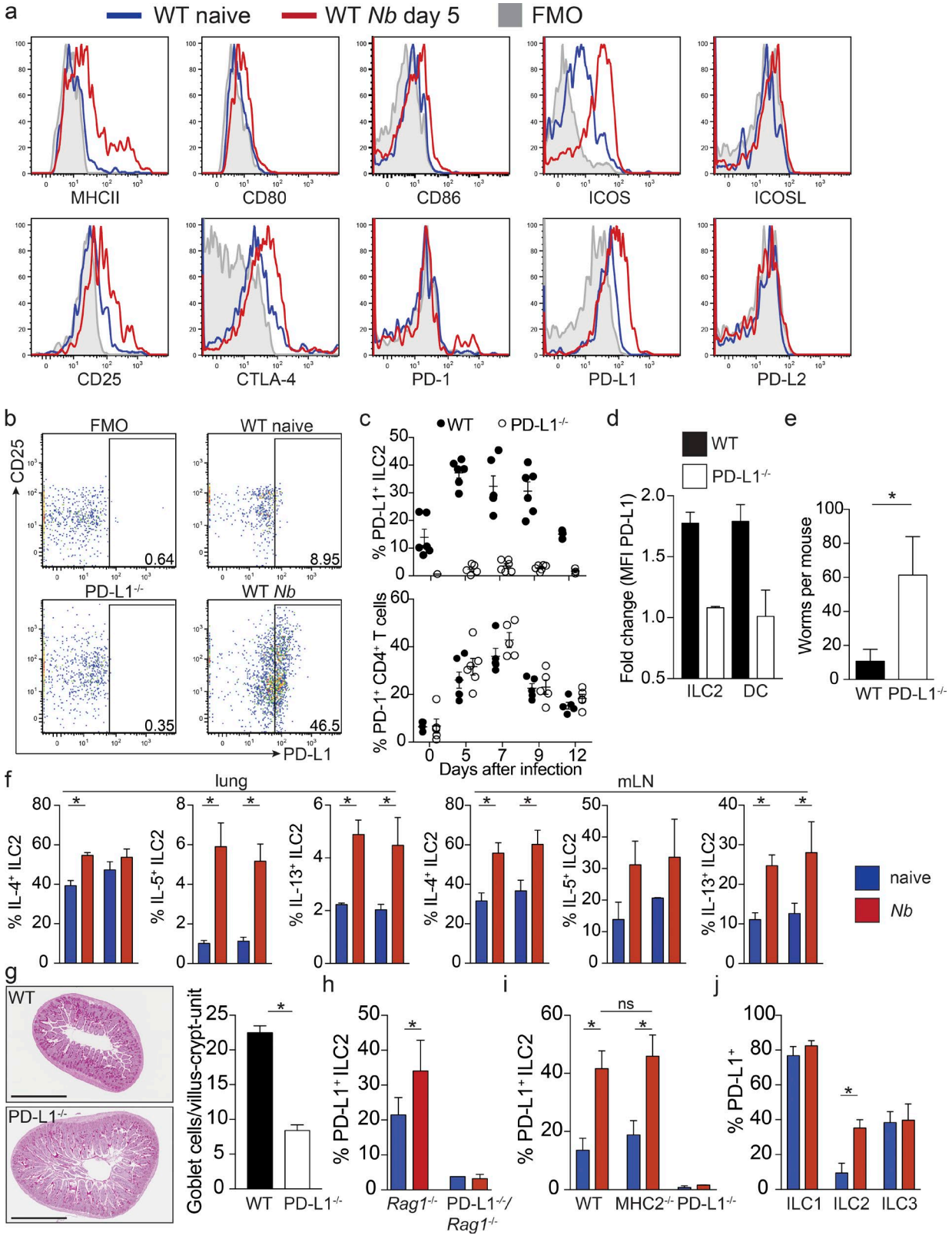

Figure 1. **PD-L1 is expressed on ILC2s and is involved in the immune response against *N. brasiliensis*.** (a) Lung lin$^-$CD45$^+$CD90$^+$ST2$^+$KLRG1$^+$ ILC2 (for gating strategy, see Fig. S1) were analyzed for surface expression of MHC II and costimulatory molecules before (blue line) and 5 d after infection with *N. brasiliensis* (*Nb*, red line) and compared with fluorescence minus one (FMO; tinted gray). (b) Dot plots show expression of PD-L1–expressing lung ILC2s

In the present study, we used the gastrointestinal helminth model *Nippostrongylus brasiliensis*, a potent inducer of ILC2s (Neill et al., 2010), to address a new mechanism of ILC2 activation of type 2 responses. After infection through the skin, *N. brasiliensis* migrates to the lung and, after passing through the stomach, lives in the small intestine, where the subsequent generation of the strong type 2 immune response in the lung and intestine mediates IL-13–dependent worm expulsion (Camberis et al., 2003). During primary infection, ILC2s are the most important initial effector cell type mediating the expulsion of the worms through several mechanisms, such as Tuft and goblet cell activation, Th2 differentiation and dendritic cell maturation, cytokine release, and initiation of tissue repair mechanisms through the activation of alternatively activated macrophages (Oliphant et al., 2014; Oeser et al., 2015; Halim et al., 2016; von Moltke et al., 2016). Here, we discovered that ILC2s can dynamically express PD-L1 and, through interaction with T cells, promote early GATA3 up-regulation, which paves the way for a robust adaptive anti-helminth Th2 cell–mediated response. These results highlight the importance of PD-L1–expressing ILC2s as an innate checkpoint for adaptive Th2 polarization and provide new insights into PD-L1–mediated activation of T cells and type 2 immunity.

RESULTS AND DISCUSSION

Identification of a PD-L1–expressing ILC2 population

Recent work has shown that ILC2s enhance the immune response against *N. brasiliensis* by instigating an MHC II–dependent dialog with CD4 T cells (Oliphant et al., 2014). Unlike the anti-inflammatory function of ILC3s (Hepworth et al., 2015), which lack the expression of canonical costimulatory molecules, ILC2s do express CD80, CD86, ICOS, ICOS-L, and KLRG-1 (Fallon et al., 2006; Neill et al., 2010; Oliphant et al., 2014; Maazi et al., 2015). For ICOS and its ligand ICOS-L, it has been described that they are required for optimal activity of ILC2s during airway inflammation (Maazi et al., 2015). We sought to identify whether other costimulatory molecules were expressed by ILC2s during their initial expansion and before the adaptive type 2 immune response is induced (Voehringer et al., 2004; Neill et al., 2010). WT mice were infected with *N. brasiliensis*, and up-regulation of costimulatory markers on ILC2s was analyzed (Figs. 1 a and S1, a and b). We observed up-regulation of MHC II molecules, CD25, ICOS, and ICOS-L on ILC2s, as reported (Oliphant et al., 2014; Maazi et al., 2015). PD-1 was up-regulated on a small subset of lung ILC2s after *N. brasiliensis* infection (Fig. 1 a), albeit to a lesser extent than reported recently (Yu et al., 2016; Taylor et al., 2017). PD-L1, but not PD-L2, was highly up-regulated on all ILC2s during the course of infection (Fig. 1, a–c). PD-L1 deficiency did not influence expression of other costimulatory molecules on ILC2s (Fig. S1 b). PD-L1 was not expressed by ILC2 progenitors (Fig. S1 c), as recently reported (Yu et al., 2016). A time course analysis of lung-resident ILC2s revealed the highest expression of PD-L1 5 d after infection, coincident with the peak of ILC2 activity and PD-1 expression on CD4 T cells in this model, with decreased frequency of PD-L1$^+$ ILC2s after the resolution of the innate immune response when the adaptive response develops with the expansion of Th2 cells (Fig. 1 c). The level of up-regulation of PD-L1 expression on ILC2s from infected mice was comparable to that of activated DCs (Figs. 1 d and S1 d). Natural ILC2s (lin$^-$CD45$^+$Thy1$^+$Sca-1$^+$ST2$^+$KLRG1^{int}) were the major ILC2 population expanding during *N. brasiliensis* infection, consistent with earlier findings (Huang et al., 2015), with natural ILC2s preferentially up-regulating PD-L1 (Fig. S1 e). Of note, PD-L1 up-regulation is not a mouse strain–specific or helminth infection–specific phenomenon, as mice on a BALB/c background increase PD-L1 expression on ILC2s after *N. brasiliensis* infection (Fig. S1 f), and increased PD-L1-expression on ILC2s was also observed after papain-induced lung inflammation (Fig. S1 g).

PD-L1 is required for worm expulsion

To address the relevance of PD-L1–mediated costimulation during type 2 immune responses, we infected WT and PD-L1–deficient *Cd274*$^{-/-}$ (PD-L1$^{-/-}$) mice with *N. brasiliensis*. PD-L1–deficient mice exhibited higher worm burdens 7 d after infection, when WT mice had largely cleared the infection (Figs. 1 e and S1 h). PD-L1 deficiency did not impair the

in WT C57BL/6 before and after infection with *N. brasiliensis* in comparison with FMO control and PD-L1$^{-/-}$ control. (c) Graphs depict PD-L1 expression on lung ILC2s and PD-1–expressing lung CD4$^+$ T cells on indicated days after *N. brasiliensis* infection in individual C57BL/6 (closed circles) and PD-L1$^{-/-}$ (open circles) mice. Mean ± SEM from three experiments is depicted. (d) Bar graph shows fold up-regulation of the mean fluorescence intensity of PD-L1 on lung ILC2s and DCs from *N. brasiliensis*–infected mice in relation to untreated controls. Bar graph shows the mean + SEM of four mice per group from two experiments. (e) Intestinal worm burden in C57BL/6 (black bar) and PD-L1$^{-/-}$ (open bar) mice 7 d after *N. brasiliensis* infection. Bar graphs show the mean + SEM of nine mice per group from three independent experiments. (f) Frequency of IL-4–, IL-5–, and IL-13–expressing ILC2s in the lung and mesenteric lymph nodes of naive (blue) and Nb-infected (red, day 5) WT (left) and PD-L1$^{-/-}$ (right) mice. Bar graphs show the mean + SEM from six mice per group from two experiments. (g) Periodic acid–Schiff staining of fixed small intestinal tissue 5 d after *N. brasiliensis* infection. Bar graph shows the mean + SD of four mice, with 5 crypt-villus units counted per mouse. Bars, 1 mm. (h) PD-L1 expression on lung ILC2s in naive and day 5 *N. brasiliensis*–infected *Rag1*$^{-/-}$ and PD-L1$^{-/-}$/*Rag1*$^{-/-}$ mice. Bar graphs show the mean + SEM from four to six mice per group from two experiments. (i) PD-L1 expression on lung ILC2s in naive and day 5 *N. brasiliensis*–infected C57BL/6, MHC2$^{-/-}$, and PD-L1$^{-/-}$ mice. Bar graphs show the mean + SD from three mice per group. (j) Small intestines from C57BL/6 mice were digested before and 5 d after infection with *N. brasiliensis*. ILC1s, ILC2s, and ILC3s were analyzed for PD-L1 expression. Bar graphs show the mean + SD from three individual mice per group. Student's *t* test was used to analyze data, and p-values <0.05 were considered statistically significant. *, $P < 0.05$; ns, not significant.

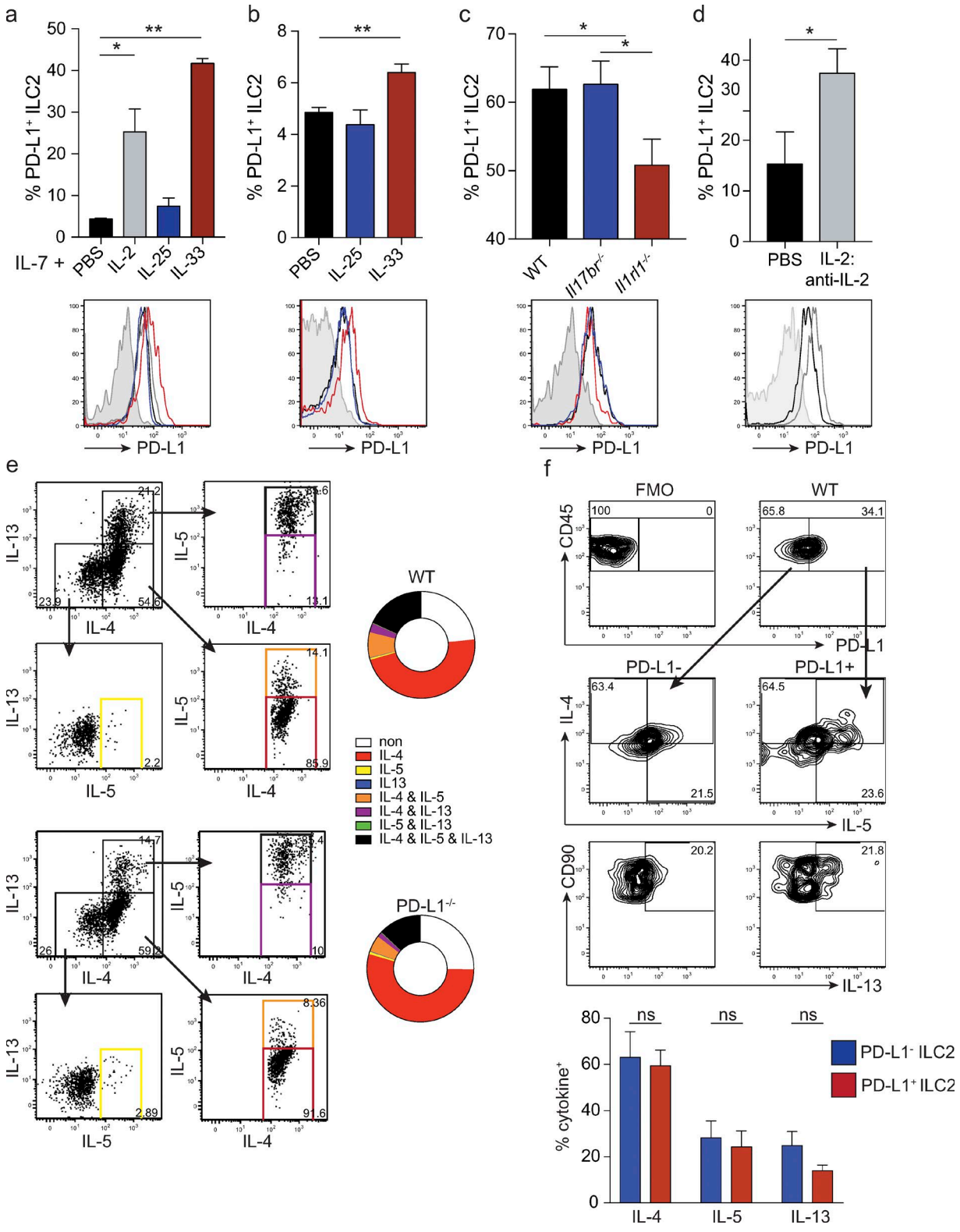

Figure 2. **PD-L1 is up-regulated on IL-33–activated ILC2s in vitro and in vivo.** (a) ILC2s were sort-purified from lungs of C57BL/6 mice and cultured in cRPMI in the presence of indicated cytokines (10 ng/ml each) for 5 d. Bar graphs show the mean + SEM of five replicates per group from two independent experiments. Histogram overlay shows representative PD-L1 expression on ILC2s. (b) C57BL/6 mice were injected i.p. with PBS, IL-25 (500 µg/dose), or IL-33 (500 µg/dose) on three consecutive days, and lung ILC2s were analyzed for PD-L1 expression the next day. Bars show the mean + SD from three mice per

production of type 2 cytokines from ILC2s (Fig. 1 f). The delay in worm expulsion may be the result of diminished generation of a functional type 2 immunity that mediates worm rejection, known as weep and sweep (Anthony et al., 2007), as illustrated by the significantly ($P < 0.05$) reduced intestinal goblet cell hyperplasia and mucus production in PD-L1$^{-/-}$ mice relative to WT mice (Fig. 1 g). Importantly, the impaired immune response is not caused by altered expansion of ILC2s or CD4$^+$ T cells in the lungs of PD-L1$^{-/-}$ mice (Fig. S1, i and j) or the ILC2 inhibitory cytokines IFNγ and IL-27 (not depicted). Because the receptor PD-1 is predominantly expressed on T cells, we were interested in whether PD-L1 expression on ILC2s is dependent on contact with cells of the adaptive immune system. Upon *N. brasiliensis* infection, ILC2s in *Rag1*$^{-/-}$ mice had up-regulated PD-L1 compared with naive controls and dual PD-L1$^{-/-}$/*Rag1*$^{-/-}$ mice (Fig. 1 h). T cell– and MHC2-independent up-regulation of PD-L1 on ILC2s was further confirmed in *N. brasiliensis*–infected MHC2$^{-/-}$ mice, which lack CD4$^+$ T cells (Fig. 1 i). Therefore, we conclude that helminth infection leads to an early innate activation of a PD-L1–expressing ILC2 population. Of note, group 1 and group 3 ILC subpopulations express PD-L1 in the steady state (Fig. 1 j). However, PD-L1 was up-regulated only on ILC2s, predominantly in the lung, during helminth infection, and we therefore focused on addressing roles of PD-L1 expression on pulmonary ILC2 function during early events of the infection.

Activation of ILC2s up-regulates PD-L1

To further delineate the requirements for PD-L1 expression on ILC2s, we isolated ILC2s and expanded them in vitro with various known ILC2 activators (Moro et al., 2015). IL-7, which is required for in vitro survival of ILCs, did not alter PD-L1 expression on ILC2s. Addition of IL-2 or IL-33 led to a significant increase in surface PD-L1 expression in ILC2s, with IL-33 being the more potent inducer, whereas IL-25 did not have an effect on PD-L1 expression (Fig. 2 a). Injection of WT mice with recombinant cytokines confirmed the selective up-regulation of PD-L1 on ILC2s in response to IL-33, but not IL-25 (Fig. 2 b). Conversely, infection of mice deficient in the receptors for IL-33 or IL-25 demonstrated that PD-L1 up-regulation was ablated only in the absence of IL-33–mediated ST2 signaling (Fig. 2 c). Additionally, in vivo expansion of ILC2s after injection of IL-2:anti-IL-2 complexes into *Rag1*$^{-/-}$ mice further confirmed the up-regulation of PD-L1 expression on activated ILC2s (Fig. 2 d). These data demonstrate that activation of lung ILC2s leads to increased surface expression of PD-L1.

In light of the recent finding that ILC2 progenitors expressed PD-1 (Yu et al., 2016), we investigated whether deficiency in PD-L1 affected cytokine expression by ILC2s because of a lack of PD-1:PD-L1 interactions during ILC2 development. We expanded ILC2s in vitro and analyzed production of IL-4, IL-5, and IL-13 by flow cytometry (Fig. 2 e). Interestingly, the majority of ILC2s produced IL-4 in vitro, with only a few single producers of IL-5 or IL-13. Their capacity to produce IL-5 and IL-13 has been investigated in depth and accounts for most of their effector functions. Although ILC2s were discovered in IL-4 reporter mice (Fallon et al., 2006), their relative contribution to the innate-derived IL-4 pool is less clear (Pelly et al., 2016). However, there was no difference between ILC2s generated from WT or PD-L1$^{-/-}$ mice regarding their expression of type 2 cytokines (Fig. 2 e). Analysis of PD-L1$^+$ and PD-L1$^-$ ILC2s in *N. brasiliensis*–infected WT mice revealed no significant alterations in the proportions of type 2 cytokine producers in the two compartments (Fig. 2 f). Because PD-L1$^+$ and PD-L1$^-$ ILC2s did not differ in their ability to produce type 2 cytokines in vitro and in vivo, we concluded that the delayed worm rejection in PD-L1–deficient mice was not caused by an inability of ILC2s to produce the key worm rejection effector cytokine IL-13. Therefore, we sought to determine whether PD-L1$^+$ ILC2s could directly influence CD4$^+$ T cells.

PD-L1–mediated PD-1 engagement leads to Th2 polarization

It has been shown that ILC2s enter a dialog with T cells in the context of *N. brasiliensis* infection, which ultimately leads to an increase of IL-13 produced from T cells (Oliphant et al., 2014). We co-cultured naive CD4$^+$ T cells alone or together with ILC2s from WT or PD-L1$^{-/-}$ mice to determine whether the absence of a PD-L1 checkpoint signal on ILC2s leads to uncontrolled T cell differentiation and type 2 immunopathology. Surprisingly, PD-L1–expressing ILC2s stimulated CD4 T cells under nonpolarizing conditions to significantly increase GATA3 protein expression and IL-13 production (Figs. 3 a and S2 a). Importantly, interference with PD-1:PD-L1 interaction during differentiation did not affect

group from one of two independent experiments. Histogram overlay shows representative PD-L1 expression on ILC2s. (c) WT, *Il17br*$^{-/-}$, and *Il1rl1*$^{-/-}$ mice were infected with *N. brasiliensis* and analyzed for PD-L1–expressing lung ILC2s 5 d later. Bars show the mean + SEM from 5–10 mice per group from two independent experiments. Histogram overlay shows representative PD-L1 expression on ILC2s. (d) *Rag1*$^{-/-}$ mice were injected with IL-2:anti–IL-2 complexes three times every other day, and lung ILC2s were analyzed for PD-L1 expression 2 d later. Bars show the mean + SD from at least two individual mice per group. Histogram overlay shows representative PD-L1 expression on ILC2s. (e) ILC2s were isolated from lungs of naive WT and PD-L1$^{-/-}$ mice, expanded in vitro for 5 d (IL-2, IL-7, and IL-33; 10 ng/ml each), stimulated for the final 5 h with PMA/ionomycin in the presence of monensin, and stained intracellularly for IL-4, IL-5, and IL-13. Plots are gated on live lin$^-$CD90$^+$KLRG1$^+$ST2$^+$ cells. FMO, fluorescence minus one. (f) Bar graph shows the mean + SEM IL-4, IL-5, and IL-13 producers within the PD-L1$^-$ and PD-L1$^+$ population within the ILC2s from lungs of nine *N. brasiliensis*–infected WT mice from two experiments. Contour plots show representative gating of PD-L1$^-$ and PD-L1$^+$ cells and flow cytometric signal for intracellular IL-4, IL-5, and IL-13. Student's *t* test was used to analyze data, and p-values <0.05 were considered statistically significant. *, $P < 0.05$; **, $P < 0.01$; ns, not significant.

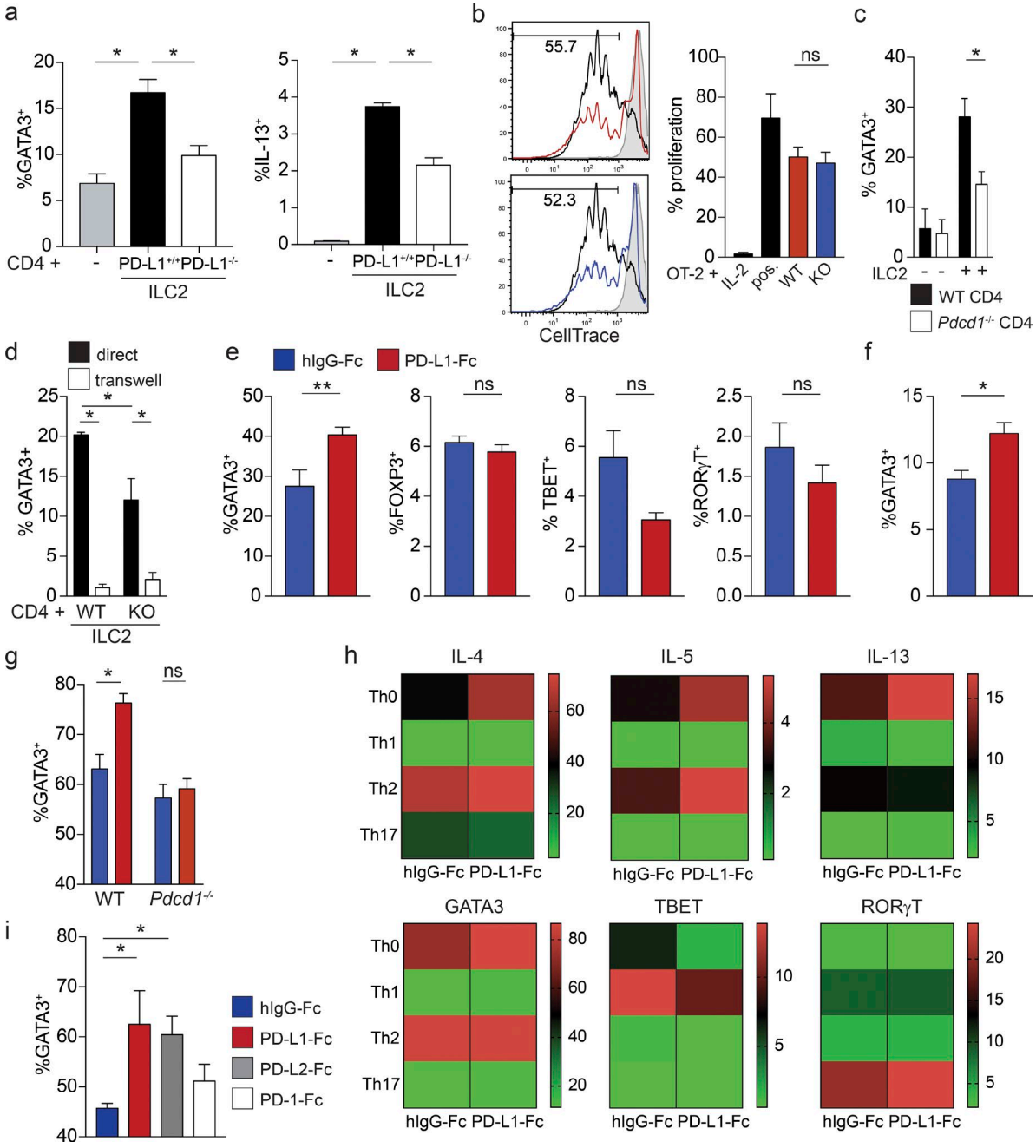

Figure 3. **PD-L1:PD-1 interaction promotes Th2 polarization in CD4 T cells in vitro.** (a) Sort-purified ILC2s from the lungs of day 5 *N. brasiliensis*–infected WT (PD-L1 expression: see Fig. 1 c, day 5, top) and PD-L1$^{-/-}$ mice and naive WT CD3$^+$CD4$^+$CD44$^-$ T cells (PD-1 expression: see Fig. 1 c, day 0, bottom) were co-cultured (or T cells only) for 5 d. GATA3 expression in T cells was analyzed by intranuclear staining. Cells were restimulated with PMA/ionomycin, and IL-13 was stained intracellularly and analyzed by flow cytometry. Bar graphs show the mean + SEM of 13 and four to eight independent replicates from three experiments, respectively. (b) Purified naive, CellTrace Violet–labeled OT-2 T cells were cultured for 5 d in the presence of IL-2 (20 ng/ml), anti-CD3/anti-CD28 (5 µg/ml/1 µg/ml; "pos."), WT ILC2 + OVA (10 µg/ml), or PD-L1$^{-/-}$ ILC2 + OVA (10 µg/ml). Histograms show the dilution of CellTrace Violet in CD4$^+$ T cells. Bar graph shows the mean + SEM of six samples from two experiments. (c) WT or *Pdcd1*$^{-/-}$ CD4$^+$ T cells were cultured alone or together with WT ILCs as in a. Bar graph shows the mean + SEM of six replicates. (d) Cells were co-cultured as in a in Transwell or normal plates ("direct" cell–cell contact). Bar graph shows the mean + SEM of six samples from two experiments. (e) Purified naive CD4 T cells were cultured under nonpolarizing conditions for 24 h in the presence of anti-CD3 antibody (5 µg/ml) with recombinant mouse PD-L1-Fc (5 µg/ml; red bars) or control protein (5 µg/ml; blue bars). Cells were stained intranuclearly for indicated transcription factors. Bar graphs show the mean + SEM of four to nine replicates from three experiments. (f) T cells from IL-4Ra$^{-/-}$ mice were cultured as in e. Bar graph shows the mean + SEM of five replicates from two experiments. (g) Naive T cells from WT and *Pdcd1*$^{-/-}$ mice were cultured as described in e and analyzed for GATA3 expression 24 h later. Bars show the mean + SEM of five replicates. (h) WT CD4 T cells

the ability to present antigen via MHC II or increase cell death of T cells in the co-cultures (Figs. 3 b and S2 b). Furthermore, in our ILC2:CD4 T cell co-culture system, GATA3 up-regulation was dependent on PD-1 expression on CD4 T cells and direct cell–cell contact (Fig. 3, c and d). To confirm the effect of PD-L1 on CD4 T cell polarization, recombinant PD-L1 chimeric fusion protein, in which mouse PD-L1 is fused to the Fc portion of human IgG1 (PD-L1-Fc), was used to ligate PD-1 on T cells (McAlees et al., 2015). Purified naive T cells cultured in the presence of anti-CD3 antibody and PD-L1-Fc, or human IgG1 control, up-regulated GATA3 protein (Figs. 3 e and S2, c and d) in a manner that operates independently of IL-4– and IL-13–mediated signaling via IL-4Rα (Fig. 3 f). Of note, the expression of FOXP3, RORγt, and TBET on Th cells was not significantly altered by PD-L1-Fc stimulation (Fig. 3 e). Furthermore, stimulation of naive $CD4^+$ T cells isolated from PD-1–deficient *Pdcd1*$^{-/-}$ mice with PD-L1-Fc did not increase GATA3 expression (Fig. 3 g). As a consequence of the increased early GATA3 expression, PD-L1–stimulated T cells produced more IL-4, IL-5, and IL-13 under nonpolarizing (Th0), as well as Th2-polarizing, conditions (Figs. 3 h and S2 e). In contrast, the presence of PD-L1-Fc under Th17-polarizing conditions did not alter cytokine expression. Similar to PD-L1-Fc, stimulation with PD-L2-Fc (but not PD-1-Fc) led to an increase in GATA3 expression (Fig. 3 i). In summary, we provide direct evidence that PD-L1 selectively induces Th0 cells to differentiate into Th2-polarized cells.

PD-L1–mediated costimulatory activity has been reported previously (Bennett et al., 2003; McAlees et al., 2015), and recently it has been found that PD-L1 and PD-L2 compete for binding to PD-1 on T cells during experimental *Plasmodium* infection (Karunarathne et al., 2016). Here, PD-L1:PD-1 interactions inhibit Th1 cell responses, whereas PD-L2 on DCs prevents T cell inhibition. In contrast to *N. brasiliensis*, control of acute malarial parasitemia is dependent on IFNγ-producing T cells and highlights the dynamic regulation of T helper subsets via PD-1. That PD-L1 and PD-L2 can have differential effects when binding to PD-1 present on CD4 T cells was described more than a decade ago (Dong et al., 1999), and more recent studies show different conformational changes when PD-1 interacts with PD-L1 or PD-L2 (Ghiotto et al., 2010). Studies showing an inhibitory function rely on Th1- or Th17-biased models. During *S. mansoni* infections, PD-L1 is up-regulated on macrophages, inhibiting IFNγ-producing T cell responses (Smith et al., 2004). Although PD-L1 is up-regulated on macrophages in the presence of IFNγ, IL-4 up-regulates PD-L2 expression, reflecting the segregation of the negative feedback loops between Th1 and Th2 responses (Loke and Allison, 2003; Huber et al., 2010; Ishiwata et al., 2010).

It is currently not clear what leads to the increased expression of GATA3 in naive CD4 T cells upon PD-1 engagement. Possible explanations include T-bet down-regulation, which can repress GATA3 (Usui et al., 2006); decreased TCR signaling strength, which favors Th2 differentiation (Constant et al., 1995) and full T cell activation (Valitutti et al., 1995; Hansen et al., 2011); STAT modulation (Amarnath et al., 2011); and shifts in the mTOR complex balance (Yang et al., 2013), or combinations thereof. Depending on the cytokine microenvironment, PD-1 signaling modulates the signals received by the CD4 T cells and shifts the balance toward activating differentiation (Th2 and Treg) or inhibiting proliferation (Th1 and Th17). Herein, we show that PD-L1 engagement of PD-1 on naive $CD4^+$ cells preferentially expands Th2 cells in vitro.

Expression of PD-L1 on ILC2s enhances Th2 polarization

To test whether PD-L1:PD-1-mediated ILC2–T cell interactions observed in vitro (Fig. 3 a) were functionally relevant in vivo, we transferred naive CD4 T cells alone or together with PD-$L1^{+/+}$ and PD-$L1^{-/-}$ ILC2s into *Rag2*$^{-/-}\gamma_c^{-/-}$ mice deficient in ILCs and T and B cells and infected the mice with *N. brasiliensis* to expand Th2 cells. Mice receiving PD-L1–deficient ILC2s—with disrupted ILC2–T cell dialog—had a significantly impaired ability to mount an efficient type 2 immune response after infection, as indicated by a significant decrease in $GATA3^+$ Th2 cells and eosinophils, leading to reduced ability to expel worms (Fig. 4, a–d). Importantly, transfer of PD-L1–expressing ILC2s together with *Pdcd1*$^{-/-}$ CD4 T cells abrogated protective immunity (Fig. 4, c and d). This confirms that ILC2 expression of PD-L1 mediates Th2 cell expansion in vivo.

ILC2-specific deletion of PD-L1 impairs anti-helminth response

Although adoptive transfers of ILCs into *Rag2*$^{-/-}\gamma_c^{-/-}$ have become a standard procedure assessing the functional role of ILC2s, it remains an artificial system, which lacks almost all components of the innate and adaptive immune system and does not formally address ILC2-specific functions. We therefore generated a novel mouse with a loxP-flanked *Cd274* gene (PD-$L1^{fl/fl}$; Fig. S3, a and b). Successful excision by a ubiquitously expressed Cre recombinase ($ActinB^{Cre}$) of the first two coding exons including the start codon leads to the complete absence of PD-L1 from the surface

were cultured for 5 d under nonpolarizing and Th1-, Th2-, and Th17-polarizing conditions in the presence or absence of recombinant PD-L1 and analyzed for indicated transcription factors and cytokines. Heat maps depict means of six replicates. Bar graphs are shown in Fig. S2. (i) Naive WT CD4 T cells were cultured under nonpolarizing conditions in the presence of control recombinant hIgG-Fc, PD-L1-Fc, PD-L2-Fc, or PD-1-Fc (5 µg/ml each) and analyzed for GATA3 expression by flow cytometry 24 h later. Bars show the mean + SEM of six replicates. Student's *t* test was used to analyze data, and p-values <0.05 were considered statistically significant. *, $P < 0.05$; **, $P < 0.01$; ns, not significant.

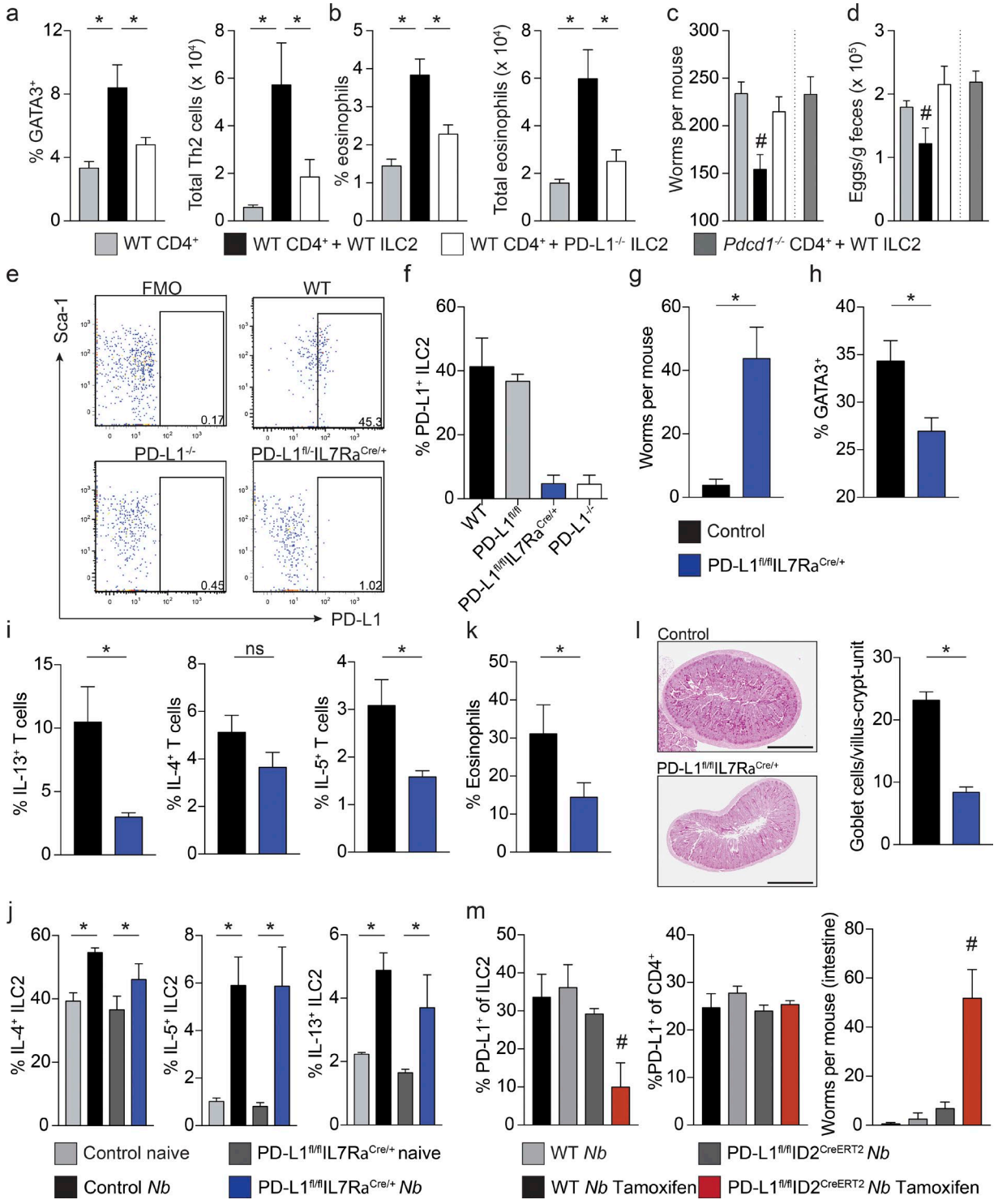

Figure 4. **PD-L1–expressing ILC2s control the PD-1 checkpoint toward Th2 polarization during helminth infection.** (a) *Rag2*$^{-/-}$*Il2rg*$^{-/-}$ mice received naive CD4 T cells alone or together with WT or PD-L1$^{-/-}$ ILC2s and were infected with *N. brasiliensis* the next day. Lungs were analyzed for GATA3^{+} CD4 T cells and eosinophils (b) by flow cytometry. Bar graphs show the mean + SEM of five individual mice per group from two independent experiments. (c) Intestinal worm burden and fecal egg counts (d) 7 d after infection in mice receiving CD4 T cells alone (light gray), WT CD4 T cells and PD-L1$^{+/+}$ (black bars) or PD-L1$^{-/-}$ (open bars) ILC2s, or *Pdcd1*$^{-/-}$ CD4 T cells and WT ILC2s (dark gray). Bars show the mean + SEM of four to nine mice per group from three experiments. (e) Representative dot plots showing the PD-L1 expression on lung ILC2s (gated on live lin^{-}CD45^{+}CD90^{+}ST2^{+}KLRG1^{+} cells) from infected WT, PD-L1$^{-/-}$ and PDL1$^{fl/-}$IL7Rα$^{Cre/+}$ mice 5 d after infection. FMO, fluorescence minus one. (f) PD-L1 expression on lung ILC2s in WT, PD-L1$^{fl/fl}$, PD-L1$^{-/-}$, and PDL-

(Fig. S3 b). By crossing PD-L1$^{fl/fl}$ mice to mice expressing Cre within the ILC population (*IL7Ra*^{Cre}), we efficiently knocked down PD-L1 expression on ILC2s to levels found in a PD-L1$^{-/-}$ mouse (Fig. 4, e and f). Mice with a disruption of the PD-1:PD-L1 crosstalk between T cells and ILC2s had significantly impaired *N. brasiliensis* worm rejection (Figs. 4 g and S3 c). Expulsion of *N. brasiliensis* is critically dependent on CD4 T cells and IL-13 production (Barner et al., 1998; Urban et al., 1998). Consistent with the absence of a functional type 2 response to mediate worm expulsion, CD4$^+$ T cell expression of GATA3 was decreased in conditional ILC-PD-L1 knockout mice compared with control mice (Fig. 4 h), with a significant decrease in IL-13– and IL-5–expressing CD4 T cells, but not ILC2s (Fig. 4, i and j; and Fig. S3 d). Expulsion during the primary infection is critically dependent on IL-4 and IL-13 and T cells (Voehringer et al., 2006); however, T cell–derived IL-4/13 is dispensable for worm expulsion by day 9 but required for the recruitment of other effector cells such as eosinophils, basophils, and ILC2s (Oeser et al., 2015). Indeed, we observed a decrease in eosinophils in both PD-L1$^{fl/-}$IL7Rα$^{Cre/+}$ and PD-L1$^{-/-}$ mice (Fig. 4 k and not depicted). Further, we observed significantly impaired intestinal activation in PD-L1$^{fl/-}$IL7Rα$^{Cre/+}$ mice after infection (Fig. 4 l). A recent study has shown that DCs up-regulate PD-L1 after *N. brasiliensis* infection in an IFNα/β receptor (IFNAR)–dependent manner (Connor et al., 2017); however, our conditional knockout did not alter PD-L1 expression on DC. Yet we do not exclude the possibility that there is a function for PD-L1–mediated activation by DCs in certain immune states.

A tissue-specific checkpoint control mechanism that governs Th2 differentiation during *N. brasiliensis* infection has been described (Van Dyken et al., 2016). Others have shown that during *N. brasiliensis* infection, T cells can be polarized toward Th2 in a Stat6- and IL-4–independent manner (van Panhuys et al., 2008). Our study identifies a novel mechanism whereby PD-L1–expressing ILC2s function as a pulmonary checkpoint of Th2 differentiation.

As we had used an IL7RαCre, which deletes PD-L1 also on T cells, it is important to point out that the immune response against *N. brasiliensis* was intact in PD-L1$^{fl/-}$CD4$^{Cre/+}$, confirming no role for PD-L1 expression on T cells in this model (Fig. S3, e–g). To further restrict PD-L1 deficiency to the ILC lineage, we generated PD-L1$^{fl/fl}$ID2Cre^{ERT2} mice. Tamoxifen administration induced specific knockdown of PD-L1 expression in ILC2s but not other cell types (Figs. 4 m and S3 h). We confirmed that treatment with tamoxifen did not interfere with the immune response of WT mice against *N. brasiliensis,* and only tamoxifen-treated PD-L1$^{fl/fl}$ID2Cre^{ERT2} mice, unlike their untreated littermates, exhibited increased worm burdens (Fig. 4 m). Finally, we investigated whether PD-1 was required for an efficient immune response against *N. brasiliensis*. Although the infection was cleared in *Pdcd1*$^{-/-}$ mice, up-regulation of GATA3 in CD4 T cells was impaired to the same extent as observed in PD-L1$^{-/-}$ mice; however, cytokine production by *Pdcd1*$^{-/-}$ ILC2s was enhanced, accounting for the accelerated worm clearance (Fig. S3, i and j). These results are in line with recent articles describing PD-1 as an important developmental inhibitor of ILC2s (Yu et al., 2016; Taylor et al., 2017). During reinfections, we did not observe a contribution of PD-L1 to the immune response (unpublished data), which was to be expected because other T cell–independent mechanisms have been shown to be responsible for the elimination of *N. brasiliensis* before they complete their life cycle in previously infected mice—namely antibodies, basophils, eosinophils, and macrophages (Knott et al., 2007; Chen et al., 2014; Schwartz et al., 2014). Collectively, our results demonstrate that PD-L1 expression on pulmonary ILC2s is critically required to fully instruct CD4 T cells to differentiate into IL-13–producing Th2 effector cells. Although ILC2s are capable to induce naive CD4 T cells to differentiate to Th2 cells in vitro and also after adoptive cell transfer in vivo, in a natural infection ILC2s are more likely to interact with primed T cells within the lung, where PD-L1:PD-1 interaction represents a checkpoint for the further activation of effector Th2 functions.

Concluding remarks

With the present study, we have discovered a new mechanism by which ILC2s regulate T cell fate and demonstrate a novel activating role of PD-L1 costimulation during helminth infections. This activating function of PD-1 engagement is of particular interest because it will have consequences during cancer treatment assessment (Ribas and Hu-Lieskovan, 2016). Treatment of PD-L1$^+$ cancers with blocking anti–PD-1 or anti–PD-L1 antibodies may lead to adverse side effects, such as psoriasis, colitis, or pneumonia (Postow, 2015). In light of

1$^{fl/-}$IL7Rα$^{Cre/+}$ mice. Bar graphs show the mean + SD of at least three mice per group. (g) Control and PDL1$^{fl/-}$IL7Rα$^{Cre/+}$ mice were infected with *N. brasiliensis*, and worm burden was analyzed 7 d after infection. Bar graph shows the mean + SEM of nine mice from three experiments. (h) Th2 cell IL-4-, IL-5-, and IL-13 production (i) in lung CD4 T cells or ILC2s (j) and lung eosinophil infiltration (k) were analyzed by flow cytometry 5 d after infection. Bar graphs show the mean + SEM of six to 10 mice from three independently performed experiments. (l) Periodic acid–Schiff staining of fixed small intestinal tissue 5 d after *N. brasiliensis* infection. Bar graph shows the mean + SD of three mice, with 5 crypt-villus units counted per mouse. Bars, 1 mm. (m) WT or PDL1$^{fl/fl}$ID2^{CreERT2} mice were left untreated or injected i.p. with tamoxifen before infection with *N. brasiliensis*. Bar graphs show the mean + SEM of PD-L1 expression on lung ILC2s (left) and CD4 T cells (middle) and worm burden 7 d after infection (right) from at least three mice per group from two experiments. Student's *t* test was used to analyze data, and p-values <0.05 were considered statistically significant. *, P < 0.05, ns, not significant. In c, d, and m, ANOVA was used to determine statistical significance. #, P < 0.01.

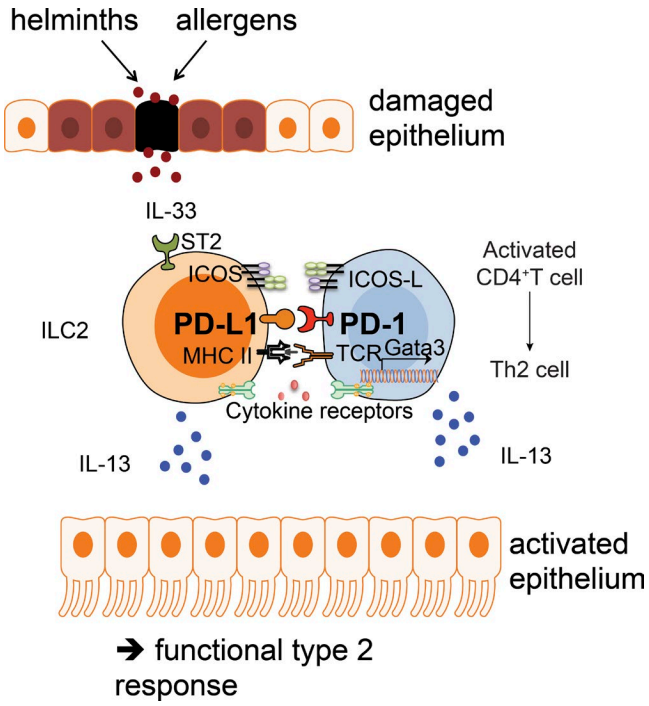

Figure 5. **Working model.** Helminth- or allergen-inflicted epithelial damage leads to the release of IL-33, which activates ILC2s via ST2. ILCs up-regulate PD-L1 and interact with CD4 T cells on site to promote increased GATA3 expression and thereby commit them to IL-13–producing Th2 cells. IL-13 released from both cell types then activates the epithelium to promote worm expulsion.

our data, this may be a consequence of altering the maintenance of the Th2 response in skin, lung, and intestine in favor of empowering the Th1 response and therefore leading to immunopathology. Indeed, PD-1 blockade in patients with prostate and advanced melanoma enhances Th1 and Th17 responses at the cost of suppressing Th2 responses (Dulos et al., 2012). As we have observed, IL-33 up-regulates PD-L1 on ILC2s, and a similar pathway may up-regulate PD-L1 in different cancers. This is particularly important because ST2 expression and high IL-33 levels are associated with worse prognosis (Mertz et al., 2015).

In summary, we have identified that PD-L1 expression on ILC2 mediates innate CD4 T cell dialog within the lung to checkpoint adaptive Th2 polarization, leading to a more robust functional type 2 immune response that mediates worm expulsion (Fig. 5). However, it still remains to be shown how pulmonary interactions affect intestinal worm clearance, and although we think it is likely that similar mechanisms govern ILC2:CD4 T cell interactions in the intestinal tract, this needs to be investigated in more detail. This novel ILC2-controlled differentiation checkpoint governs the Th2 response to ultimately break the helminth life cycle but may also have important implications during allergic type 2–mediated inflammatory diseases.

MATERIALS AND METHODS

Study design

Groups of age- and sex-matched mice were infected with the gastrointestinal helminth *N. brasiliensis*. Parameters analyzed included flow cytometric analysis of lung tissue, serum antibody concentrations, and determination of worm numbers in the small intestines of experimental animals. In the study, *n* refers to the number of animals used in any particular experiment or the number of individual replicates (in vitro). All experiments were repeated at least once.

Mice

*Cd274*loxP (PD-L1$^{fl/fl}$) mice were generated on a B6 background by Taconic Biosciences according to the targeting strategy described in Fig. S3. In brief, LoxP sites were introduced by homologous recombination flanking the start codon and the first two coding exons (exons 2 and 3) of *Cd274*. C57BL/6J mice were originally obtained from the Jackson Laboratory, and a colony is maintained on site. B7-H1$^{-/-}$ (PD-L1$^{-/-}$) mice were originally obtained from L. Chen (Yale University, New Haven, CT) and maintained on a C57BL/6 background. *Il7r*$^{tm1.1(icre)Hrr}$ (IL7Rα^{Cre}) mice were as described (Schlenner et al., 2010). B6-*Rag2*^{tm1Fwa} *Il2rg*^{tm1Wjl} (*Rag2*$^{-/-}\gamma_c^{-/-}$) and B6.129S6-*Rag2*^{tm1Fwa} Tg(Tcra-Tcrb)425Cbn were purchased from Taconic Biosciences. *Id2*$^{tm1.1(cre/ERT2)Blh}$ (Rawlins et al., 2009) and *Pdcd1*$^{-/-}$ (Keir et al., 2007) mice were purchased from the Jackson Laboratory. *Il4ra*^{tm1Sz} (Noben-Trauth et al., 1997) were obtained from the Jackson Laboratory and backcrossed to B6 background for >12 generations. *Il1rl1*^{tm1Anjm} (ST2$^{-/-}$), *Il17br*$^{-/-}$, and *MHC2*$^{-/-}$ were previously described (Cosgrove et al., 1991; Townsend et al., 2000; Neill et al., 2010). Animals were housed in a specific pathogen–free facility in individually ventilated cages under positive pressure. Mice had ad libitum access to food and water. All animal experiments were performed in compliance with Irish Medicines Board/Health Products Regulatory Authority regulations and approved by the Trinity College Dublin's BioResources ethics review board.

N. brasiliensis infection

N. brasiliensis is maintained by passage through Wistar rats. Mice 6–8 wk of age were injected subcutaneously with 500 live infective L3-stage *N. brasiliensis* larvae and killed by cervical dislocation for analysis at the indicated time points after infection.

Tissue preparation and flow cytometry

Lungs were flushed with PBS before extraction to remove blood cells. Lungs were minced and incubated with 100 µg/ml collagenase I (Roche) for 30 min at 37°C. Single-cells suspension were obtained through filtering through a 100-µm (lungs) or 70-µm (lymph nodes and spleens) cell strainer (BD). For the preparation of cells from the small intestine, mesenteric fat and Peyer's patches were removed before the small intestine was longitudinally cut open and incubated

with shaking (200 rpm) at 37°C in HBSS containing 5% FBS and 5 mM EDTA for 30 min. After extensive washing to remove EDTA, the tissue was minced and incubated with shaking (200 rpm) at 37°C in HBSS containing 5% FBS, 1.6 mg/ml collagenase D (Roche), and 40 µg/ml DNaseI (Sigma-Aldrich) for 45 min. Digested tissue was filtered through a 100-µm cell strainer and washed in HBSS containing 5% FBS before staining for flow cytometric analysis. Cells were then stained with Live/Dead aqua (Life Technologies) in PBS for 30 min at 4°C, and Fc receptors were blocked with 10 µg/ml purified anti-CD16/32 antibody (clone 93; eBioscience) in FACS buffer (PBS, 2% FBS, and Na_3N) for 15 min at 4°C. After washing with FACS buffer, the cells were stained with the following antibodies (all eBioscience unless stated otherwise): eFluor 450 (e450)-conjugated lineage cocktail (CD3 [17A2], TCRb [H57-597], CD5 [53-7.3], CD19 [ebio1D3], γδ TCR [ebioGL3], CD11b [M1/70], CD11c [N418], FcERIa [MAR-1], Ter-119 [TER-119], Gr-1 [RB6-8C5], and F4/80 [BM8]), allophycocyanin (APC)-conjugated lineage cocktail (CD3 [17A2], TCRβ [H57-597], CD5 [53-7.3], CD19 [ebio1D3], γδ TCR [ebioGL3], CD11b [M1/70], CD11c [HL3], FcERIα [MAR-1], Ter-119 [TER-119], Gr-1 [RB6-8C5], and F4/80 [BM8]), FITC-conjugated anti-T1/ST2 (clone DJ8; MD Biosciences), PE- or APC-conjugated anti-CD274 (MIH5), PE-e610–conjugated anti-KLRG1 (2F1), APC-conjugated anti-CD25 (PC61.5), PE-Cy7–conjugated anti-Ly6A/E (D7; BD), PerCP-Cy5.5–conjugated anti-ICOS (7E.17G9; BD), PerCP-Cy5.5– or PE-CF594–conjugated anti-CD45 (30-F11 and 104; BD), FITC- or PE-conjugated anti–PD-L2 (122), FITC- or PE-conjugated anti–PD-1 (RMP1-30), PE- or APC-conjugated anti–Siglec-F (E50-2440; BD), PerCP-Cy5.5– or APC-e780–conjugated anti-IL7Rα/XΔ127 (eBioSB/199), e450- or APC-e780–conjugated anti-MHC2 (M5/114.15.2), PE-CF594–conjugated anti-CD80 (16-10A1; BD), FITC-conjugated anti-CD86 (GL1; BD), PE-conjugated anti-ICOSL (B7RP.1), PE-conjugated anti-CD152/CTLA4 (UC10-4B9), APC-, PE-e610–, or FITC-conjugated anti-CD3 (145-2C11 and 17A2), APC-, APC-e780–, or PerCP-Cy5.5–conjugated anti-CD4 (RM4-5), FITC-conjugated anti-CCR3 (J073E5; BioLegend), PerCP-Cy5.5–conjugated anti-CD11b (M1/70), PE-Cy7– or e450-conjugated anti-CD11c (N418), PE-Texas Red–conjugated anti-NKp46 (29A1.4), FITC- or APC-conjugated anti-F4/80 (BM8), and PE-Cy7– or e660-conjugated anti-CD206 (C068C2; BioLegend). ILC1s were defined as $Lin^-CD45^+IL\text{-}7R\alpha^+CD90^+ST2^-NKp46^+ROR\gamma t^-$, ILC2s as $Lin^-CD45^+IL\text{-}7R\alpha^+CD90^+ST2^+NKp46^-ROR\gamma t^-$ or $Lin^-CD45^+IL\text{-}7R\alpha^+CD90^+ST2^+KLRG1^+$, and ILC3s as $Lin^-CD45^+IL\text{-}7R\alpha^+CD90^+ST2^-NKp46^-ROR\gamma t^+$.

For staining of transcription factors, cells were fixed and permeabilized using the FoxP3 staining buffer kit (eBioscience) and stained with the following antibodies: PE-, PE-Cy7–, or e660-conjugated GATA3 (TWAJ), FITC- or APC-conjugated anti-Tbet (O4-46; BD), Brilliant Violet 421–conjugated anti-RORγT (Q31-378), and APC- or PE-CF594–conjugated anti-FoxP3 (MF23; BD).

For intracellular detection of cytokines, cells were stimulated with 50 ng/ml PMA (Sigma) and 1 µg/ml ionomycin (R&D Systems) for 5 h in the presence of monensin (eBioscience) for the last 3 h. After staining of surface antigens, cells were fixed and permeabilized using the BD Cytofix/Cytoperm kit (BD), and the following antibodies were used for staining: FITC- or APC-conjugated anti–IL-4 (BVD5-24G2), PE-conjugated anti–IL-5 (TRFK5; BD), APC- or PE-Cy7–conjugated anti–IL-13, PerCP-Cy5.5– or APC-conjugated anti-IFNγ (XMG1.2 and eBio13A), PE-conjugated anti-IL17A (TC11-18H10; BD), and PerCP-Cy5.5–conjugated anti–IL-9 (D9302C12; BD).

Cell sorting

ILC2s were sorted by FACS from the lungs of day 5 *N. brasiliensis*–infected mice. ILC2s identified as lineage-negative, $CD45^+ST2^+KLRG1^+IL7R\alpha^+Sca\text{-}1^+$ cells were either used directly in T cell co-cultures or subsequently expanded in cRPMI (RPMI 1640 [Gibco] supplemented with penicillin/streptavidin [Gibco], L-glutamine [Gibco], and 10% fetal bovine serum [Gibco]) containing 10 ng/ml IL-2 (R&D Systems), 10 ng/ml IL-7 (R&D Systems), and 10 ng/ml IL-33 (R&D Systems) for 5 d.

For in vitro activation studies, lineage-negative cells were sorted by magnetic-activated cell sorting (MACS). Cells were labeled with lineage-APC antibodies and anti–APC-microbeads (Miltenyi Biotec) in MACS buffer (PBS, 2 mM EDTA, and BSA [all Sigma-Aldrich]) according to the manufacturer's instructions and separated using an AutoMACS system (Miltenyi Biotec). Cells were then cultured in the presence of cytokines for 7 d to generate >95% pure ILC2 cultures. T cells (>95% purity) were isolated from the spleens of naive mice using the mouse CD4 T cell isolation kit according to the manufacturer's instructions. For OT-2 co-cultures, T cells were isolated from $Rag2^{+/-}OT\text{-}2^{tg/+}$ mice, stained with CellTrace Violet (Molecular Probes) according to the manufacturer's protocol, and incubated with ILC2s and OVA protein (10 µg/ml) for 5 d.

Adoptive transfers

ILC2s were isolated from the lungs of *N. brasiliensis*–infected WT or $PD\text{-}L1^{-/-}$ mice and expanded in vitro as previously described (Neill et al., 2010). Purified splenic $CD4^+CD44^-$ T cells were freshly isolated from naive donors. $Rag2^{-/-}Il2rg^{-/-}$ mice were injected intravenously with 8×10^5 CD4 T cells and 2×10^5 ILC2s 1 d before infection with *N. brasiliensis*.

Tamoxifen treatment

Mice were injected three times i.p. with 75 mg/kg body weight tamoxifen (Sigma-Aldrich) dissolved in oil and rested for 1 wk after the final injection before they were infected with *N. brasiliensis*.

Cell culture

Sorted $CD3^+CD4^+CD44^-$ T cells from naive donor mice were cultured on plates coated with 5 µg/ml anti-CD3 and 5 µg/ml recombinant chimeric PD-L1-Fc-fusion protein, recombinant chimeric PD-L2-Fc-fusion protein, recombinant chimeric PD-1-Fc-fusion protein, or human IgG1 control protein (all R&D Systems). Cells were analyzed for the expression of transcription factors and cytokines 24 and 96 h later, respectively.

Th differentiation was achieved through the culture of naive CD4 T cells in the presence of polarizing cytokines for 5 d as previously described. Plates were precoated with 5 µg/ml anti-CD3 (2C11) and PD-L1-Fc or control protein, and cells were cultured in cRPMI containing 2 µg/ml anti-CD28. Nonpolarizing Th0 conditions: 20 ng/ml IL-2; Th1, IL-2, IFNγ, and anti–IL-4; Th2, IL-2, IL-4, and anti–IL-12; Th17, IL-6, TGFβ, anti–IL-4, and anti-IFNγ; and Treg, IL-2, TGFβ, anti–IL-4, and anti-IFNγ.

Histology

Small intestine tissue was fixed in 10% neutral buffered formalin and embedded in paraffin, and 4-µm slices were cut on a microtome before staining with periodic acid–Schiff reagent. Pictures were acquired on an Aperio ScanScope.

Postacquisition and statistical analysis

Flow cytometric data were analyzed using FlowJo software (v8.8.7; Tree Star). GraphPad Prism (v7) was used to generate graphs and for statistical analysis. Student's *t* test and ANOVA were used to determine statistical significance. P-values <0.05 were considered statistically significant.

Online supplemental material

Fig. S1 (related to Fig. 1) shows ILC2 gating strategy; supporting flow cytometry plots for ILC progenitors, dendritic cells, iILC2s, and nILCs; and kinetics of worm clearance in WT and PD-$L1^{-/-}$ mice. Fig. S2 (related to Fig. 3) shows representative flow cytometry plots and supporting information for cell culture experiments. Fig. S3 (related to Fig. 4) shows the construct for the generation of PD-L1loxP mice and efficiency of deletion, worm clearance kinetics of WT and conditional knockout mice, and *N. brasiliensis* infection of PD-$L1^{fl/fl}CD4^{Cre/+}$ and *Pdcd1*$^{-/-}$ mice.

ACKNOWLEDGMENTS

C. Schwartz is a Long-Term EMBO Fellow (ALTF 587-2016). P.G. Fallon was supported by Science Foundation Ireland (10/IN.1/B3004), the Wellcome Trust (092530/Z/10/Z), and National Children's Research Centre.

The authors declare no competing financial interests.

Author contributions: C. Schwartz designed, performed and analyzed experiments and wrote the manuscript; A.R. Khan, A. Floudas, S.P. Saunders, and E. Hams performed or contributed to specific experiments; H-R. Rodewald and A.N.J. McKenzie provided essential reagents; P.G. Fallon conceptualized the study, designed and supervised the experiments, analyzed data, and wrote the manuscript.

Submitted: 9 January 2017
Revised: 2 June 2017
Accepted: 5 July 2017

REFERENCES

Agata, Y., A. Kawasaki, H. Nishimura, Y. Ishida, T. Tsubata, H. Yagita, and T. Honjo. 1996. Expression of the PD-1 antigen on the surface of stimulated mouse T and B lymphocytes. *Int. Immunol.* 8:765–772. http://dx.doi.org/10.1093/intimm/8.5.765

Amarnath, S., C.W. Mangus, J.C. Wang, F. Wei, A. He, V. Kapoor, J.E. Foley, P.R. Massey, T.C. Felizardo, J.L. Riley, et al. 2011. The PDL1-PD1 axis converts human TH1 cells into regulatory T cells. *Sci. Transl. Med.* 3:111ra120. http://dx.doi.org/10.1126/scitranslmed.3003130

Anthony, R.M., L.I. Rutitzky, J.F. Urban Jr., M.J. Stadecker, and W.C. Gause. 2007. Protective immune mechanisms in helminth infection. *Nat. Rev. Immunol.* 7:975–987. http://dx.doi.org/10.1038/nri2199

Barber, D.L., E.J. Wherry, D. Masopust, B. Zhu, J.P. Allison, A.H. Sharpe, G.J. Freeman, and R. Ahmed. 2006. Restoring function in exhausted CD8 T cells during chronic viral infection. *Nature.* 439:682–687. http://dx.doi.org/10.1038/nature04444

Barner, M., M. Mohrs, F. Brombacher, and M. Kopf. 1998. Differences between IL-4R alpha-deficient and IL-4-deficient mice reveal a role for IL-13 in the regulation of Th2 responses. *Curr. Biol.* 8:669–672. http://dx.doi.org/10.1016/S0960-9822(98)70256-8

Bennett, F., D. Luxenberg, V. Ling, I.M. Wang, K. Marquette, D. Lowe, N. Khan, G. Veldman, K.A. Jacobs, V.E. Valge-Archer, et al. 2003. Program death-1 engagement upon TCR activation has distinct effects on costimulation and cytokine-driven proliferation: Attenuation of ICOS, IL-4, and IL-21, but not CD28, IL-7, and IL-15 responses. *J. Immunol.* 170:711–718. http://dx.doi.org/10.4049/jimmunol.170.2.711

Camberis, M., G. Le Gros, and J. Urban Jr. 2003. Animal model of *Nippostrongylus brasiliensis* and *Heligmosomoides polygyrus*. *Curr. Protoc. Immunol.* Chapter 19:Unit 19.12. http://dx.doi.org/10.1002/0471142735.im1912s55

Chen, F., W. Wu, A. Millman, J.F. Craft, E. Chen, N. Patel, J.L. Boucher, J.F. Urban Jr., C.C. Kim, and W.C. Gause. 2014. Neutrophils prime a long-lived effector macrophage phenotype that mediates accelerated helminth expulsion. *Nat. Immunol.* 15:938–946. http://dx.doi.org/10.1038/ni.2984

Connor, L.M., S.C. Tang, E. Cognard, S. Ochiai, K.L. Hilligan, S.I. Old, C. Pellefigues, R.F. White, D. Patel, A.A. Smith, et al. 2017. Th2 responses are primed by skin dendritic cells with distinct transcriptional profiles. *J. Exp. Med.* 214:125–142. http://dx.doi.org/10.1084/jem.20160470

Constant, S., C. Pfeiffer, A. Woodard, T. Pasqualini, and K. Bottomly. 1995. Extent of T cell receptor ligation can determine the functional differentiation of naive CD4+ T cells. *J. Exp. Med.* 182:1591–1596. http://dx.doi.org/10.1084/jem.182.5.1591

Cosgrove, D., D. Gray, A. Dierich, J. Kaufman, M. Lemeur, C. Benoist, and D. Mathis. 1991. Mice lacking MHC class II molecules. *Cell.* 66:1051–1066. http://dx.doi.org/10.1016/0092-8674(91)90448-8

del Rio, M.L., G. Penuelas-Rivas, R. Dominguez-Perles, P. Ramirez, P. Parrilla, and J.I. Rodriguez-Barbosa. 2005. Antibody-mediated signaling through PD-1 costimulates T cells and enhances CD28-dependent proliferation. *Eur. J. Immunol.* 35:3545–3560. http://dx.doi.org/10.1002/eji.200535232

Dong, H., G. Zhu, K. Tamada, and L. Chen. 1999. B7-H1, a third member of the B7 family, co-stimulates T-cell proliferation and interleukin-10 secretion. *Nat. Med.* 5:1365–1369. http://dx.doi.org/10.1038/70932

Dulos, J., G.J. Carven, S.J. van Boxtel, S. Evers, L.J. Driessen-Engels, W. Hobo, M.A. Gorecka, A.F. de Haan, P. Mulders, C.J. Punt, et al. 2012. PD-1 blockade augments Th1 and Th17 and suppresses Th2 responses in

peripheral blood from patients with prostate and advanced melanoma cancer. *J. Immunother.* 35:169–178. http://dx.doi.org/10.1097/CJI.0b013e318247a4e7

Fallon, P.G., S.J. Ballantyne, N.E. Mangan, J.L. Barlow, A. Dasvarma, D.R. Hewett, A. McIlgorm, H.E. Jolin, and A.N. McKenzie. 2006. Identification of an interleukin (IL)-25-dependent cell population that provides IL-4, IL-5, and IL-13 at the onset of helminth expulsion. *J. Exp. Med.* 203:1105–1116. http://dx.doi.org/10.1084/jem.20051615

Flach, M., and A. Diefenbach. 2015. Adipose tissue: ILC2 crank up the heat. *Cell Metab.* 21:152–153. http://dx.doi.org/10.1016/j.cmet.2015.01.015

Fort, M.M., J. Cheung, D. Yen, J. Li, S.M. Zurawski, S. Lo, S. Menon, T. Clifford, B. Hunte, R. Lesley, et al. 2001. IL-25 induces IL-4, IL-5, and IL-13 and Th2-associated pathologies in vivo. *Immunity.* 15:985–995. http://dx.doi.org/10.1016/S1074-7613(01)00243-6

Freeman, G.J., A.J. Long, Y. Iwai, K. Bourque, T. Chernova, H. Nishimura, L.J. Fitz, N. Malenkovich, T. Okazaki, M.C. Byrne, et al. 2000. Engagement of the PD-1 immunoinhibitory receptor by a novel B7 family member leads to negative regulation of lymphocyte activation. *J. Exp. Med.* 192:1027–1034. http://dx.doi.org/10.1084/jem.192.7.1027

Ghiotto, M., L. Gauthier, N. Serriari, S. Pastor, A. Truneh, J.A. Nunès, and D. Olive. 2010. PD-L1 and PD-L2 differ in their molecular mechanisms of interaction with PD-1. *Int. Immunol.* 22:651–660. http://dx.doi.org/10.1093/intimm/dxq049

Gorski, S.A., Y.S. Hahn, and T.J. Braciale. 2013. Group 2 innate lymphoid cell production of IL-5 is regulated by NKT cells during influenza virus infection. *PLoS Pathog.* 9:e1003615. http://dx.doi.org/10.1371/journal.ppat.1003615

Halim, T.Y., R.H. Krauss, A.C. Sun, and F. Takei. 2012. Lung natural helper cells are a critical source of Th2 cell-type cytokines in protease allergen-induced airway inflammation. *Immunity.* 36:451–463. http://dx.doi.org/10.1016/j.immuni.2011.12.020

Halim, T.Y., Y.Y. Hwang, S.T. Scanlon, H. Zaghouani, N. Garbi, P.G. Fallon, and A.N. McKenzie. 2016. Group 2 innate lymphoid cells license dendritic cells to potentiate memory T2 cell responses. *Nat. Immunol.* 17:57–64. http://dx.doi.org/10.1038/ni.3294

Hansen, A.K., M. Regner, C.M. Bonefeld, L. Boding, M. Kongsbak, N. Ødum, A. Müllbacher, C. Geisler, and M.R. von Essen. 2011. TCR down-regulation boosts T-cell-mediated cytotoxicity and protection against poxvirus infections. *Eur. J. Immunol.* 41:1948–1957. http://dx.doi.org/10.1002/eji.201141413

Hepworth, M.R., L.A. Monticelli, T.C. Fung, C.G. Ziegler, S. Grunberg, R. Sinha, A.R. Mantegazza, H.L. Ma, A. Crawford, J.M. Angelosanto, et al. 2013. Innate lymphoid cells regulate CD4+ T-cell responses to intestinal commensal bacteria. *Nature.* 498:113–117. http://dx.doi.org/10.1038/nature12240

Hepworth, M.R., T.C. Fung, S.H. Masur, J.R. Kelsen, F.M. McConnell, J. Dubrot, D.R. Withers, S. Hugues, M.A. Farrar, W. Reith, et al. 2015. Immune tolerance. Group 3 innate lymphoid cells mediate intestinal selection of commensal bacteria-specific $CD4^+$ T cells. *Science.* 348:1031–1035. http://dx.doi.org/10.1126/science.aaa4812

Huang, Y., L. Guo, J. Qiu, X. Chen, J. Hu-Li, U. Siebenlist, P.R. Williamson, J.F. Urban Jr., and W.E. Paul. 2015. IL-25-responsive, lineage-negative KLRG1(hi) cells are multipotential 'inflammatory' type 2 innate lymphoid cells. *Nat. Immunol.* 16:161–169. http://dx.doi.org/10.1038/ni.3078

Huber, S., R. Hoffmann, F. Muskens, and D. Voehringer. 2010. Alternatively activated macrophages inhibit T-cell proliferation by Stat6-dependent expression of PD-L2. *Blood.* 116:3311–3320. http://dx.doi.org/10.1182/blood-2010-02-271981

Ishiwata, K., N. Watanabe, M. Guo, K. Tomihara, M.J. Brumlik, H. Yagita, D. Pardoll, L. Chen, and T. Shin. 2010. Costimulator B7-DC attenuates strong Th2 responses induced by *Nippostrongylus brasiliensis*. *J. Immunol.* 184:2086–2094. http://dx.doi.org/10.4049/jimmunol.0804051

Karunarathne, D.S., J.M. Horne-Debets, J.X. Huang, R. Faleiro, C.Y. Leow, F. Amante, T.S. Watkins, J.J. Miles, P.J. Dwyer, K.J. Stacey, et al. 2016. Programmed death-1 ligand 2-mediated regulation of the PD-L1 to PD-1 axis is essential for establishing CD4(+) T cell immunity. *Immunity.* 45:333–345. http://dx.doi.org/10.1016/j.immuni.2016.07.017

Keir, M.E., G.J. Freeman, and A.H. Sharpe. 2007. PD-1 regulates self-reactive CD8+ T cell responses to antigen in lymph nodes and tissues. *J. Immunol.* 179:5064–5070. http://dx.doi.org/10.4049/jimmunol.179.8.5064

Keir, M.E., M.J. Butte, G.J. Freeman, and A.H. Sharpe. 2008. PD-1 and its ligands in tolerance and immunity. *Annu. Rev. Immunol.* 26:677–704. http://dx.doi.org/10.1146/annurev.immunol.26.021607.090331

Khan, A.R., E. Hams, A. Floudas, T. Sparwasser, C.T. Weaver, and P.G. Fallon. 2015. PD-L1hi B cells are critical regulators of humoral immunity. *Nat. Commun.* 6:5997. http://dx.doi.org/10.1038/ncomms6997

Kim, B.S., M.C. Siracusa, S.A. Saenz, M. Noti, L.A. Monticelli, G.F. Sonnenberg, M.R. Hepworth, A.S. Van Voorhees, M.R. Comeau, and D. Artis. 2013. TSLP elicits IL-33-independent innate lymphoid cell responses to promote skin inflammation. *Sci. Transl. Med.* 5:170ra16. http://dx.doi.org/10.1126/scitranslmed.3005374

Klose, C.S., and D. Artis. 2016. Innate lymphoid cells as regulators of immunity, inflammation and tissue homeostasis. *Nat. Immunol.* 17:765–774. http://dx.doi.org/10.1038/ni.3489

Knott, M.L., K.I. Matthaei, P.R. Giacomin, H. Wang, P.S. Foster, and L.A. Dent. 2007. Impaired resistance in early secondary *Nippostrongylus brasiliensis* infections in mice with defective eosinophilopoeisis. *Int. J. Parasitol.* 37:1367–1378. http://dx.doi.org/10.1016/j.ijpara.2007.04.006

Latchman, Y., C.R. Wood, T. Chernova, D. Chaudhary, M. Borde, I. Chernova, Y. Iwai, A.J. Long, J.A. Brown, R. Nunes, et al. 2001. PD-L2 is a second ligand for PD-1 and inhibits T cell activation. *Nat. Immunol.* 2:261–268. http://dx.doi.org/10.1038/85330

Liechtenstein, T., I. Dufait, C. Bricogne, A. Lanna, J. Pen, K. Breckpot, and D. Escors. 2012. PD-L1/PD-1 co-stimulation, a brake for T cell activation and a T cell differentiation signal. *J. Clin. Cell. Immunol.* Suppl 12:006.

Loke, P., and J.P. Allison. 2003. PD-L1 and PD-L2 are differentially regulated by Th1 and Th2 cells. *Proc. Natl. Acad. Sci. USA.* 100:5336–5341. http://dx.doi.org/10.1073/pnas.0931259100

Maazi, H., N. Patel, I. Sankaranarayanan, Y. Suzuki, D. Rigas, P. Soroosh, G.J. Freeman, A.H. Sharpe, and O. Akbari. 2015. ICOS:ICOS-ligand interaction is required for type 2 innate lymphoid cell function, homeostasis, and induction of airway hyperreactivity. *Immunity.* 42:538–551. http://dx.doi.org/10.1016/j.immuni.2015.02.007

McAlees, J.W., S. Lajoie, K. Dienger, A.A. Sproles, P.K. Richgels, Y. Yang, M. Khodoun, M. Azuma, H. Yagita, P.C. Fulkerson, et al. 2015. Differential control of CD4(+) T-cell subsets by the PD-1/PD-L1 axis in a mouse model of allergic asthma. *Eur. J. Immunol.* 45:1019–1029. http://dx.doi.org/10.1002/eji.201444778

Mertz, K.D., L.F. Mager, M.H. Wasmer, T. Thiesler, V.H. Koelzer, G. Ruzzante, S. Joller, J.R. Murdoch, T. Brümmendorf, V. Genitsch, et al. 2015. The IL-33/ST2 pathway contributes to intestinal tumorigenesis in humans and mice. *OncoImmunology.* 5:e1062966. http://dx.doi.org/10.1080/2162402X.2015.1062966

Mirchandani, A.S., A.G. Besnard, E. Yip, C. Scott, C.C. Bain, V. Cerovic, R.J. Salmond, and F.Y. Liew. 2014. Type 2 innate lymphoid cells drive CD4+ Th2 cell responses. *J. Immunol.* 192:2442–2448. http://dx.doi.org/10.4049/jimmunol.1300974

Monticelli, L.A., G.F. Sonnenberg, M.C. Abt, T. Alenghat, C.G. Ziegler, T.A. Doering, J.M. Angelosanto, B.J. Laidlaw, C.Y. Yang, T. Sathaliyawala, et al. 2011. Innate lymphoid cells promote lung-tissue homeostasis after infection with influenza virus. *Nat. Immunol.* 12:1045–1054. http://dx.doi.org/10.1038/ni.2131

Monticelli, L.A., L.C. Osborne, M. Noti, S.V. Tran, D.M. Zaiss, and D. Artis. 2015. IL-33 promotes an innate immune pathway of intestinal tissue

protection dependent on amphiregulin-EGFR interactions. *Proc. Natl. Acad. Sci. USA.* 112:10762–10767. http://dx.doi.org/10.1073/pnas.1509070112

Monticelli, L.A., M.D. Buck, A.L. Flamar, S.A. Saenz, E.D. Tait Wojno, N.A. Yudanin, L.C. Osborne, M.R. Hepworth, S.V. Tran, H.R. Rodewald, et al. 2016. Arginase 1 is an innate lymphoid-cell-intrinsic metabolic checkpoint controlling type 2 inflammation. *Nat. Immunol.* 17:656–665. http://dx.doi.org/10.1038/ni.3421

Moro, K., T. Yamada, M. Tanabe, T. Takeuchi, T. Ikawa, H. Kawamoto, J. Furusawa, M. Ohtani, H. Fujii, and S. Koyasu. 2010. Innate production of T_H2 cytokines by adipose tissue-associated c-Kit$^+$Sca-1$^+$ lymphoid cells. *Nature.* 463:540–544. http://dx.doi.org/10.1038/nature08636

Moro, K., K.N. Ealey, H. Kabata, and S. Koyasu. 2015. Isolation and analysis of group 2 innate lymphoid cells in mice. *Nat. Protoc.* 10:792–806. http://dx.doi.org/10.1038/nprot.2015.047

Neill, D.R., S.H. Wong, A. Bellosi, R.J. Flynn, M. Daly, T.K. Langford, C. Bucks, C.M. Kane, P.G. Fallon, R. Pannell, et al. 2010. Nuocytes represent a new innate effector leukocyte that mediates type-2 immunity. *Nature.* 464:1367–1370. http://dx.doi.org/10.1038/nature08900

Noben-Trauth, N., L.D. Shultz, F. Brombacher, J.F. Urban Jr., H. Gu, and W.E. Paul. 1997. An interleukin 4 (IL-4)-independent pathway for CD4+ T cell IL-4 production is revealed in IL-4 receptor-deficient mice. *Proc. Natl. Acad. Sci. USA.* 94:10838–10843. http://dx.doi.org/10.1073/pnas.94.20.10838

Oeser, K., C. Schwartz, and D. Voehringer. 2015. Conditional IL-4/IL-13-deficient mice reveal a critical role of innate immune cells for protective immunity against gastrointestinal helminths. *Mucosal Immunol.* 8:672–682. http://dx.doi.org/10.1038/mi.2014.101

Oliphant, C.J., Y.Y. Hwang, J.A. Walker, M. Salimi, S.H. Wong, J.M. Brewer, A. Englezakis, J.L. Barlow, E. Hams, S.T. Scanlon, et al. 2014. MHCII-mediated dialog between group 2 innate lymphoid cells and CD4(+) T cells potentiates type 2 immunity and promotes parasitic helminth expulsion. *Immunity.* 41:283–295. http://dx.doi.org/10.1016/j.immuni.2014.06.016

Pelly, V.S., Y. Kannan, S.M. Coomes, L.J. Entwistle, D. Rückerl, B. Seddon, A.S. MacDonald, A. McKenzie, and M.S. Wilson. 2016. IL-4-producing ILC2s are required for the differentiation of TH2 cells following *Heligmosomoides polygyrus* infection. *Mucosal Immunol.* 9:1407–1417. http://dx.doi.org/10.1038/mi.2016.4

Postow, M.A. 2015. Managing immune checkpoint-blocking antibody side effects. *Am. Soc. Clin. Oncol. Educ. Book.* 35:76–83. http://dx.doi.org/10.14694/EdBook_AM.2015.35.76

Price, A.E., H.E. Liang, B.M. Sullivan, R.L. Reinhardt, C.J. Eisley, D.J. Erle, and R.M. Locksley. 2010. Systemically dispersed innate IL-13-expressing cells in type 2 immunity. *Proc. Natl. Acad. Sci. USA.* 107:11489–11494. http://dx.doi.org/10.1073/pnas.1003988107

Rawlins, E.L., C.P. Clark, Y. Xue, and B.L. Hogan. 2009. The Id2+ distal tip lung epithelium contains individual multipotent embryonic progenitor cells. *Development.* 136:3741–3745. http://dx.doi.org/10.1242/dev.037317

Ribas, A., and S. Hu-Lieskovan. 2016. What does PD-L1 positive or negative mean? *J. Exp. Med.* 213:2835–2840. http://dx.doi.org/10.1084/jem.20161462

Saenz, S.A., M.C. Siracusa, J.G. Perrigoue, S.P. Spencer, J.F. Urban Jr., J.E. Tocker, A.L. Budelsky, M.A. Kleinschek, R.A. Kastelein, T. Kambayashi, et al. 2010. IL25 elicits a multipotent progenitor cell population that promotes T(H)2 cytokine responses. *Nature.* 464:1362–1366. http://dx.doi.org/10.1038/nature08901

Salimi, M., J.L. Barlow, S.P. Saunders, L. Xue, D. Gutowska-Owsiak, X. Wang, L.C. Huang, D. Johnson, S.T. Scanlon, A.N. McKenzie, et al. 2013. A role for IL-25 and IL-33-driven type-2 innate lymphoid cells in atopic dermatitis. *J. Exp. Med.* 210:2939–2950. http://dx.doi.org/10.1084/jem.20130351

Schlenner, S.M., V. Madan, K. Busch, A. Tietz, C. Läufle, C. Costa, C. Blum, H.J. Fehling, and H.R. Rodewald. 2010. Fate mapping reveals separate origins of T cells and myeloid lineages in the thymus. *Immunity.* 32:426–436. http://dx.doi.org/10.1016/j.immuni.2010.03.005

Schwartz, C., A. Turqueti-Neves, S. Hartmann, P. Yu, F. Nimmerjahn, and D. Voehringer. 2014. Basophil-mediated protection against gastrointestinal helminths requires IgE-induced cytokine secretion. *Proc. Natl. Acad. Sci. USA.* 111:E5169–E5177. http://dx.doi.org/10.1073/pnas.1412663111

Seo, S.K., H.Y. Jeong, S.G. Park, S.W. Lee, I.W. Choi, L. Chen, and I. Choi. 2008. Blockade of endogenous B7-H1 suppresses antibacterial protection after primary *Listeria monocytogenes* infection. *Immunology.* 123:90–99. http://dx.doi.org/10.1111/j.1365-2567.2007.02708.x

Smith, P., C.M. Walsh, N.E. Mangan, R.E. Fallon, J.R. Sayers, A.N. McKenzie, and P.G. Fallon. 2004. *Schistosoma mansoni* worms induce anergy of T cells via selective up-regulation of programmed death ligand 1 on macrophages. *J. Immunol.* 173:1240–1248. http://dx.doi.org/10.4049/jimmunol.173.2.1240

Sonnenberg, G.F., and D. Artis. 2015. Innate lymphoid cells in the initiation, regulation and resolution of inflammation. *Nat. Med.* 21:698–708. http://dx.doi.org/10.1038/nm.3892

Taylor, S., Y. Huang, G. Mallett, C. Stathopoulou, T.C. Felizardo, M.A. Sun, E.L. Martin, N. Zhu, E.L. Woodward, M.S. Elias, et al. 2017. PD-1 regulates KLRG1(+) group 2 innate lymphoid cells. *J. Exp. Med.* 214:1663–1678. http://dx.doi.org/10.1084/jem.20161653

Townsend, M.J., P.G. Fallon, D.J. Matthews, H.E. Jolin, and A.N. McKenzie. 2000. T1/ST2-deficient mice demonstrate the importance of T1/ST2 in developing primary T helper cell type 2 responses. *J. Exp. Med.* 191:1069–1076. http://dx.doi.org/10.1084/jem.191.6.1069

Turner, J.E., P.J. Morrison, C. Wilhelm, M. Wilson, H. Ahlfors, J.C. Renauld, U. Panzer, H. Helmby, and B. Stockinger. 2013. IL-9-mediated survival of type 2 innate lymphoid cells promotes damage control in helminth-induced lung inflammation. *J. Exp. Med.* 210:2951–2965. http://dx.doi.org/10.1084/jem.20130071

Urban, J.F. Jr., N. Noben-Trauth, D.D. Donaldson, K.B. Madden, S.C. Morris, M. Collins, and F.D. Finkelman. 1998. IL-13, IL-4Ralpha, and Stat6 are required for the expulsion of the gastrointestinal nematode parasite *Nippostrongylus brasiliensis*. *Immunity.* 8:255–264. http://dx.doi.org/10.1016/S1074-7613(00)80477-X

Usui, T., J.C. Preiss, Y. Kanno, Z.J. Yao, J.H. Bream, J.J. O'Shea, and W. Strober. 2006. T-bet regulates Th1 responses through essential effects on GATA-3 function rather than on IFNG gene acetylation and transcription. *J. Exp. Med.* 203:755–766. http://dx.doi.org/10.1084/jem.20052165

Valitutti, S., M. Dessing, K. Aktories, H. Gallati, and A. Lanzavecchia. 1995. Sustained signaling leading to T cell activation results from prolonged T cell receptor occupancy. Role of T cell actin cytoskeleton. *J. Exp. Med.* 181:577–584. http://dx.doi.org/10.1084/jem.181.2.577

Van Dyken, S.J., J.C. Nussbaum, J. Lee, A.B. Molofsky, H.E. Liang, J.L. Pollack, R.E. Gate, G.E. Haliburton, C.J. Ye, A. Marson, et al. 2016. A tissue checkpoint regulates type 2 immunity. *Nat. Immunol.* 17:1381–1387. http://dx.doi.org/10.1038/ni.3582

van Panhuys, N., S.C. Tang, M. Prout, M. Camberis, D. Scarlett, J. Roberts, J. Hu-Li, W.E. Paul, and G. Le Gros. 2008. In vivo studies fail to reveal a role for IL-4 or STAT6 signaling in Th2 lymphocyte differentiation. *Proc. Natl. Acad. Sci. USA.* 105:12423–12428. http://dx.doi.org/10.1073/pnas.0806372105

Voehringer, D., K. Shinkai, and R.M. Locksley. 2004. Type 2 immunity reflects orchestrated recruitment of cells committed to IL-4 production. *Immunity.* 20:267–277. http://dx.doi.org/10.1016/S1074-7613(04)00026-3

Voehringer, D., T.A. Reese, X. Huang, K. Shinkai, and R.M. Locksley. 2006. Type 2 immunity is controlled by IL-4/IL-13 expression in hematopoietic non-eosinophil cells of the innate immune system. *J. Exp. Med.* 203:1435–1446. http://dx.doi.org/10.1084/jem.20052448

von Burg, N., G. Turchinovich, and D. Finke. 2015. Maintenance of immune homeostasis through ILC/T cell interactions. *Front. Immunol.* 6:416. http://dx.doi.org/10.3389/fimmu.2015.00416

von Moltke, J., M. Ji, H.E. Liang, and R.M. Locksley. 2016. Tuft-cell-derived IL-25 regulates an intestinal ILC2-epithelial response circuit. *Nature.* 529:221–225. http://dx.doi.org/10.1038/nature16161

Yang, K., S. Shrestha, H. Zeng, P.W. Karmaus, G. Neale, P. Vogel, D.A. Guertin, R.F. Lamb, and H. Chi. 2013. T cell exit from quiescence and differentiation into Th2 cells depend on Raptor-mTORC1-mediated metabolic reprogramming. *Immunity.* 39:1043–1056. http://dx.doi.org/10.1016/j.immuni.2013.09.015

Yu, Y., J.C. Tsang, C. Wang, S. Clare, J. Wang, X. Chen, C. Brandt, L. Kane, L.S. Campos, L. Lu, et al. 2016. Single-cell RNA-seq identifies a PD-1(hi) ILC progenitor and defines its development pathway. *Nature.* 539:102–106. http://dx.doi.org/10.1038/nature20105